

Simulations of Frequency-Domain Spectra: Structure-Function Relationships in Photosynthetic Pigment-Protein Complexes

Thomas Renger¹ and Volkhard May²

¹*Noyes Laboratory of Chemical Physics, Mail Code 127-72, California Institute of Technology, Pasadena, California 91125*

²*Institut für Physik, Humboldt-Universität zu Berlin, Hausvogteiplatz 5-7, D-10117 Berlin, Federal Republic of Germany*

(Received 20 September 1999)

The theory of dissipative exciton motion in chromophore complexes is applied to develop an approximate scheme for the simulation of frequency-domain linear absorption and circular dichroism. Besides lifetime broadening of the exciton lines and the inclusion of vibrational satellites in the spectra, the computations also account for static disorder. In applying the theory to a pigment protein complex of the photosynthetic light harvesting complex LHC-II of green plants the temperature dependence of linear absorption can be well reproduced.

PACS numbers: 87.15.Aa

In simulating the optical absorption of dye aggregates or chromophore complexes, one is confronted with the interplay of two distinct interactions: the coupling of electronic excitations to vibrational degrees of freedom and the interaction among the electronic excitations. Combining both couplings in a proper way should enable one to relate the absorption line shape to structural data.

To do this a sophisticated theoretical description of the absorption spectrum $I(\omega)$ is necessary. As it is well known, $I(\omega)$ can be calculated via the half-sided Fourier-transformed correlation function $D(t)$ of the optical transition dipole operators $\hat{\mu}$. An exact formula can be given if both of the following approximations are made. The interchromophore coupling is neglected and harmonic potential energy surfaces for the relevant electronic states are assumed (see, e.g., [1]). The other tractable limit is reached if one considers a set of chromophores coupled, e.g., via an electronic dipole-dipole interaction but being free of any influence of the vibrational degrees of freedom. Here, one is able to describe delocalized excitations of the Frenkel-exciton type with $I(\omega) \sim \sum_M |\mu_M|^2 \delta(\omega - \omega_M)$, where $\mu_M = \langle M | \hat{\mu} | 0 \rangle$ denotes the dipole matrix element for the transition into the (single) exciton state $|M\rangle$ with energy $\hbar\omega_M$.

Numerous approximation schemes have been developed to combine both types of interactions (see the recent paper [2] and the literature cited therein). It is the aim of this Letter to demonstrate the ability of such an approximative treatment by comparing numerical simulations with measured data. At the present time, the microscopically best characterized class of chromophore complexes (on an Ångström scale) is given by a selected number of pigment protein complexes (PPC) of photosynthetic active biological systems. PPC which contain as photoactive pigments different variants of chlorophyll molecules (Chl) and carotenoids fulfill a light harvesting function. The pigments are held in position by a scaffold of membrane-bound proteins. Energy transfer between the pigments occurs via an exciton mechanism [3].

Although these protein units contain only few pigments, and despite a large number of optical studies in the frequency as well as in the subpicosecond time domain, the understanding of microscopic processes is far from being settled. One reason for this lies in the complex role the proteins play. First, they guarantee definite distances between the pigments. Second, due to the complex protein structure the energies of the pigments will be shifted differently in dependence on their local protein environment. So-called site energies of the pigments can be introduced to take into account this energetic shift. Accordingly, when interpreting measurements an inhomogeneous distribution of site energies (static disorder) has to be taken into account. And, third, one has to include effects of dynamic disorder originated by the proteins.

To describe linear optical absorption we introduce the PPC Hamiltonian H_{PPC} which electronic part can be restricted to the (electronic) ground-state contribution $H_{\text{vib}}|0\rangle\langle 0|$ and to the single-exciton part $\sum_{M,N} [\delta_{M,N} \times (\hbar\omega_M + H_{\text{vib}}) + \Delta h_{MN}] |M\rangle\langle N|$. The use of the exciton eigenstates $|M\rangle$ is essential for the following since, only in this representation, a correct description of exciton relaxation can be achieved.

The various protein vibrations described by the coordinates Z_ξ are comprised in H_{vib} , whereas their coupling to the excitonic states is contained in a linear contribution to the single-exciton part $\Delta h_{MN} = \sum_\xi k_\xi^{(MN)} Z_\xi$. In the spirit of a normal-mode analysis of the protein vibrations, we can take H_{vib} as a collection of independent harmonic oscillators. Then, the protein vibrations enter the theory via special spectral densities.

To obtain a sufficient sophisticated expression for $I(\omega)$ which considers the dipole-dipole coupling and exciton-vibrational interaction, a partial summation will be carried out with respect to Δh_{MN} . This can be achieved by a particular density matrix approach [4]. We introduce a density operator $\hat{\sigma}$ reduced to the electronic (excitonic) subspace and obtain the dipole correlation function as $D(t) \sim \sum_M \mu_M^* \sigma_M(t)$. The density matrix $\sigma_M(t) = \langle M | \hat{\sigma}(t) | 0 \rangle$

(with initial condition $\sigma_M(0) = \mu_M$) has to be propagated according to the quantum master equation. It is of second order with respect to the exciton-vibrational coupling but nonlocal in time (non-Markovian equation):

$$\frac{\partial}{\partial t} \sigma_M(t) = -i\omega_M \sigma_M(t) - \sum_K \int_0^t d\tau C_{MK}(\tau) \sigma_K(t - \tau). \quad (1)$$

The correlation function reads $C_{MK}(\tau) = \sum_{N,\xi} \omega_\xi^2 \times k_\xi^{(MN)} k_\xi^{(NK)} \{ [n_{BE}(\omega_\xi) + 1] \exp[-i(\omega_N + \omega_\xi)\tau] + n_{BE}(\omega_\xi) \exp[-i(\omega_N - \omega_\xi)\tau] \}$, and $n_{BE}(\omega_\xi)$ denotes the Bose-Einstein distribution function of vibrational quanta. To calculate the linear absorption spectrum according to $I(\omega) \sim \sum_M \mu_M^* \text{Re} \tilde{\sigma}_M(\omega)$, we apply a half-sided Fourier transform to Eq. (1) and obtain an algebraic system of equations for the $\tilde{\sigma}_M(\omega)$. Within the so-called secular approximation [4] only the diagonal part $C_M = C_{MM}$ of the correlation function is needed and the absorption coefficient reads

$$I(\omega) \sim \left\langle \sum_M \frac{|\mu_M|^2 C_M^{\text{Re}}(\omega)}{[\omega - \omega_M - C_M^{\text{Im}}(\omega)]^2 + [C_M^{\text{Re}}(\omega)]^2} \right\rangle_{\text{conf}}. \quad (2)$$

The configuration averaging with respect to static disorder in the PPC is abbreviated by $\langle \dots \rangle_{\text{conf}}$. As a consequence of the memory terms in the density matrix Eq. (1), the line shift $C_M^{\text{Im}}(\omega)$ and the exciton line broadenings $C_M^{\text{Re}}(\omega)$ become frequency dependent. They are obtained from the correlation function of the exciton-vibrational coupling according to $C_M^{\text{Re}}(\omega) + iC_M^{\text{Im}}(\omega) = \sum_N \sum_{mn} \times K_{mn}^{(MN)} e^{-R_{mn}/R_c} C_m(\omega - \omega_N)$. The single-pigment correlation functions are denoted by $C_m(\omega)$, m counts the various pigments, and $K_{mn}^{(MN)} = a_m^{(M)} a_n^{(M)} a_m^{(N)} a_n^{(N)}$ comprises the expansion coefficients of the excitonic states. Here, we used the concept of the protein vibrations correlation radius R_c . It accounts for the vibrationally induced correlation among different sites in the PPC separated by R_{mn} [5]. $C_m(\omega)$ can be expressed by the spectral density $J_m(\omega) = \sum_\xi (\Delta_\xi^{(m)})^2 \delta(\omega - \omega_\xi)$, which contains the coupling factors $\Delta_\xi^{(m)}$ originating from the displacements $-2\Delta_\xi^{(m)}$ of the proteins potential energy surface along the (dimensionless) coordinate axis Z_ξ upon electronic excitation of the m th pigment. The amplitude of the spectral density gives the Huang-Rhys factor $S_m = \int d\omega J_m(\omega)$. The real part of the correlation function is related to the spectral density via $C_m^{\text{Re}}(\omega)/\pi\omega^2 = [1 + n_{BE}(\omega)] \times J_m(\omega) + n_{BE}(-\omega)J_m(-\omega)$ and the imaginary part follows from a Kramers-Kronig-like relation $\pi C_m^{\text{Im}}(\omega) = \mathcal{P} \int d\bar{\omega} C_m^{\text{Re}}(\bar{\omega})/(\omega - \bar{\omega})$.

In the following we will apply the approach to simulate the temperature dependent absorption of a PPC located in the light harvesting complex LHC-II of higher plants. The importance of exciton effects for the interpretation of absorption spectra of the LHC-II has been recognized

early [6,7]. Since the interaction between PPC monomers (which are arranged as trimers in the LHC-II) is weak, the absorption can be simulated in using a monomer model. From the structural investigations of [8] it is known that the LHC-II monomer contains 12 Chl. According to their arrangements in relation to the carotenoids they were tentatively assigned to 7 Chla and 5 Chlb (see Fig. 1). Also, the exact orientation of the Q_y optical transition dipole moments of the 12 Chl are unknown. Two orientations are possible for each Chl. In [9] and [10] extensive exciton simulations of global features of polarized absorption spectra and energy transfer kinetics could be used to reduce the number of possible dipole configurations from 2^{12} to 9 (for Chl assignment of Kühlbrandt *et al.*) or 15 (for a modified Kühlbrandt model in which Chla₆ changes its identity with b₅, see Fig. 1).

In Fig. 2 (upper part) the experimental absorption data of LHC-II trimers measured in [11] are shown together with our simulations using the two structural models mentioned above. A simplex algorithm has been applied to find the best simultaneous fit at three different temperatures [13]. Fortunately, no temperature dependence of any fit parameter had to be assumed. Temperature exclusively enters via the distribution $n_{BE}(\omega)$. The spectra were calculated as an average over 1000 homogeneous spectra, each obtained for a certain set of randomly generated site energies, using the mean site energies of the 12 Chl as well as the characteristics of static and dynamic disorder as fitting parameters. For both structural models a nice fit of the linear absorption experiment can be obtained. For the Kühlbrandt model the optimal dipole geometry according to our simulation is No. 3057 in Table 1 of [10], whereas

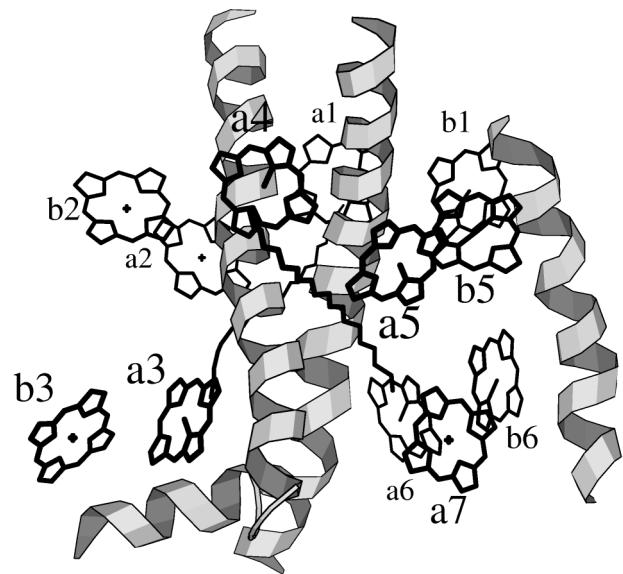


FIG. 1. Schematic cross-section view on the LHC-II monomer according to Kühlbrandt *et al.* [8]. The mutual position of the 5 Chla and 7 Chlb (shown by their tetrapyrrole ring only) is drawn together with the three α helices spanning the membrane. Graphics prepared using MOLSCRIPT [P.J. Kraulis, *J. Appl. Crystallogr.* **24**, 946 (1991)].

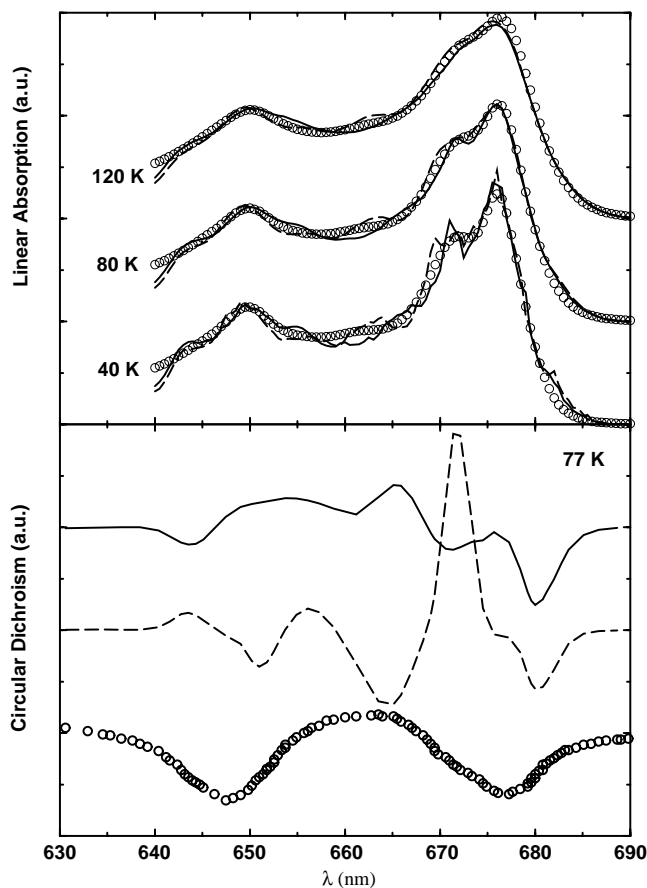


FIG. 2. Upper part: linear absorption of the LHC-II for three different temperatures within two structural models. Dashed line: Kühlbrandt model. Solid line: modified Kühlbrandt model ($\text{Chla}_6 \leftrightarrow b_5$). Circles give the experimental values of [11]. The sharp features in the 40 K spectra are due to the finite ensemble size (1000) used for the statistical average. Lower part: 77 K circular dichroism spectra within the two models compared to experimental values of [12] (circles).

the modified Kühlbrandt model favors dipole configuration No. 4004 in Table 3 of [10].

The simulations do not offer a definite decision for one of the two models. Therefore, we also simulated the circular dichroism spectra of LHC-II monomers. For the simulation, the same line shapes for the exciton transitions as in Eq. (2) can be used; however, the dipole strength $|\mu_M|^2$ has to be replaced by the rotational strength $r_M = \sum_{m>n} a_m^{(M)} a_n^{(M)} \vec{R}_{mn} (\vec{\mu}_m \otimes \vec{\mu}_n)$, where the distance (vector) between pigments m and n and the (vectorial) transition dipole moments of the pigments enter. In the lower part of Fig. 2, the 77 K circular dichroism is shown for both structural models using the parameters from the linear absorption fit. The comparison with measured data from [12] shows that only the optimized parameter set related to the modified Kühlbrandt model gives a qualitative agreement. Therefore, the subsequent discussion will be concentrated on the results obtained within this model.

According to our simulations, the inhomogeneous broadening of site energies amounts to a common value

of $\delta_{\text{pig}} = 140 \text{ cm}^{-1}$ (FWHM). As it is well-known, the resulting width δ_{exc} of the distribution of exciton energies experiences a narrowing [14] which scales with the square root of the delocalization number ($\sqrt{N_{\text{del}}} = \delta_{\text{pig}}/\delta_{\text{exc}}$). In Fig. 3 (upper part) the exciton stick spectrum obtained for the mean site energies of the pigments is shown together with the mean delocalization numbers for the various exciton levels resulting from the obtained width of the distribution of exciton energies. As a general trend the low-energetic levels exhibit a stronger delocalization than the high-energetic ones. The delocalization of the low-energetic states may increase the flexibility of the PPC to transfer excitation energy to neighboring PPC in different directions. The neglect of dynamic disorder, of course, underlines the approximative nature of this discussion.

The inhomogeneous distribution of the energy of the lowest exciton state is shown as an inset in the lower part

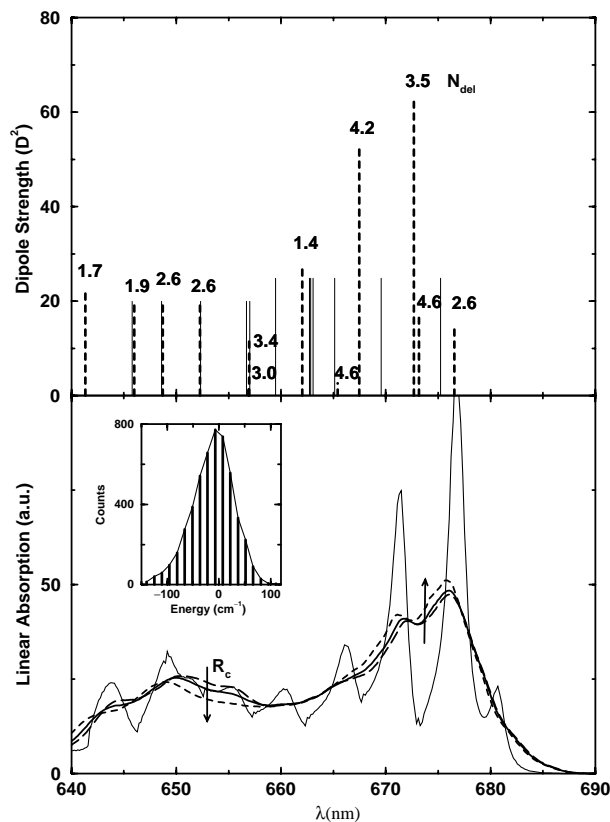


FIG. 3. Upper part: Exciton stick spectrum (dashed vertical lines) obtained for the mean site energies of the Chl (thin solid lines, from left to right: $\text{Chlb}_6, b_2, b_3, b_5, b_1, a_7, a_1, a_3, a_5, a_6, a_2, a_4$). The height of the lines gives the dipole strength of the transition, whereas the numbers at the exciton lines show the mean delocalization number of the excited state. The optimization procedure gave, for the pigment's dipole strength, values of $20D^2$ (assumed equal for all Chlb) and $25D^2$ (assumed equal for all Chla). Lower part: 80 K homogenous absorption (thin solid line) for the mean site energies and inhomogeneous absorption for different values of the correlation radius of protein vibrations: $R_c = 20 \text{ \AA}$ (solid line—same as in Fig. 2), $R_c = 2 \text{ \AA}$ (long-dashed line), and $R_c = 200 \text{ \AA}$ (short-dashed line). Inset shows the distribution of exciton energy of the lowest state.

of Fig. 3. It exhibits a width of 85 cm^{-1} . This value is in reasonable agreement with recent hole burning studies on LHC-II trimers [15] which gave 70 cm^{-1} , and additionally located the lowest exciton transition at 679.8 nm . It can be seen from the homogeneous spectrum obtained for the reference set of mean site energies (lower part of Fig. 3) that our simulation places this transition at 680 nm . Note the shift between this transition and the lowest state in the exciton stick spectrum (upper part of Fig. 3). It is caused by the imaginary part of the exciton-vibrational coupling correlation function $C_M^{\text{Im}}(\omega)$, which renormalizes the purely electronic exciton energies. Neglecting $C_M^{\text{Im}}(\omega)$ removes the shift, and, more dramatically, leads to a strong violation of the oscillator strength sum rule for different temperatures.

To keep the number of fit parameters small, we assumed the following form of the spectral density $J_m(\omega) = S_m \gamma(\omega)$, $m = \{a(\text{Ch}la), b(\text{Ch}lb)\}$. The normalized function $\gamma(\omega)$ is of the type $\gamma(\omega) \sim \omega \exp\{-(\omega/\omega_c)^p\}$. The shape of the spectral density was estimated from the fluorescence sideband at low temperatures [7], resulting in $p = 0.5$ and $\hbar\omega_c = 6 \text{ cm}^{-1}$, which put the maximum of the spectral density at $\hbar\omega = 24 \text{ cm}^{-1}$. The amplitude of the coupling, i.e., the Huang-Rhys factors determined from the fit of linear absorption amount $S_a = 0.95$ and $S_b = 0.75$. These values are not directly observable in the experiment, because they characterize the coupling of the single pigments with their protein environment, whereas the Huang-Rhys factors which are usually estimated from hole burning spectra must be related to the coupling of the excitonic states to the vibrations. To give an estimate for the relation between the two types of factors it is necessary to construct potential energy surfaces of the exciton states. This can be done by using the diagonal parts Δh_{MM} of the exciton vibrational coupling. The Huang-Rhys factor of the M th exciton state then follows from the exciton representation $S_M = \sum_{mn} |a_m^{(M)}|^2 |a_n^{(M)}|^2 e^{-R_{mn}/R_c} S_m$. In complete agreement with hole burning studies [15] we obtain for the lowest exciton state $S_{M=1} = 0.8$. As explained above, the exciton-vibrational coupling is also influenced by the correlation radius R_c of protein vibrations, for which we obtained $R_c = 20 \text{ \AA}$. In the lower part of Fig. 3 the 80 K absorption spectra are shown for two additional values of R_c (200 and 2 \AA). There is a redistribution of oscillator strength in dependence on R_c .

The standard theory of an electronic two-level system coupled to a harmonic oscillator reservoir has been applied in [16] to study the red wing of the LHC-II absorption and fluorescence in dependence on temperature. This model can be understood as dealing with a single excitonic potential energy surface. But it neglects any coupling between different potential energy surfaces, which restricts its applicability to low temperatures and the lowest exciton level [17].

In summary, we can state that our model, which is only of intermediate complexity (since it circumvents any electronic structure calculations), gives promising results in simulating the optical response of a biological important PPC. From a more general point of view our theory offers a proper way of including protein induced static and dynamic disorder which are important for the broadening of the absorption cross section of the PPC.

One of us (T.R.) would like to acknowledge support from the Alexander von Humboldt Foundation.

-
- [1] S. Mukamel, *Principles of Nonlinear Optical Spectroscopy* (Oxford, New York, 1995).
 - [2] V. Chernyak, W.M. Zhang, and S. Mukamel, *J. Chem. Phys.* **109**, 9587 (1998).
 - [3] R. van Grondelle *et al.*, *Biochim. Biophys. Acta* **1187**, 1 (1994).
 - [4] V. May and O. Kühn, *Charge and Energy Transfer Dynamics in Molecular Systems: A Theoretical Introduction* (Wiley-VCH, Berlin, 1999).
 - [5] Th. Renger and V. May, *J. Phys. Chem. A* **102**, 4381 (1998).
 - [6] P.W. Hemelrijk *et al.*, *Biochim. Biophys. Acta* **1098**, 159 (1992).
 - [7] J. Voigt *et al.*, *Phys. Status Solidi B* **194**, 333 (1996).
 - [8] W. Kühlbrandt, D.N. Wang, and Y. Fujiyoshi, *Nature (London)* **367**, 614 (1994).
 - [9] D. Gülen, R. van Grondelle, and H. van Amerongen, *J. Phys. Chem.* **101**, 7256 (1997).
 - [10] C.C. Gradinaru *et al.*, *Biophys. J.* **75**, 3046 (1998).
 - [11] J. Voigt and Th. Schrötter, *Z. Phys. Chem.* **211**, 181 (1999), Pt. 2.
 - [12] S. Nussberger *et al.*, *Biochemistry* **33**, 14775 (1994).
 - [13] The optimization procedure was organized in the following way. For each dipole configuration a set of several hundred randomly chosen start simplexes were optimized in the high-dimensional parameter space by minimizing the sum over squared deviations between experimental and simulation data. Finally, the best optimized subsets of the different geometries were compared. The two chosen optimal dipole geometries gave an about 50% smaller least square function than the remaining geometries. For a description of the simplex algorithm, see W.H. Press *et al.*, *Numerical Recipes in Fortran* (Cambridge University, Cambridge, England, 1992).
 - [14] E.W. Knapp, *Chem. Phys.* **85**, 73 (1984).
 - [15] J. Pieper *et al.*, *J. Phys. Chem. A* **103**, 2412 (1999).
 - [16] E.J.G. Peterman *et al.*, *J. Phys. Chem. B* **101**, 4448 (1997).
 - [17] Within the two-level system theory, the homogeneous fluorescence line shape can be written as $F(\omega) \propto e^{-G(0)} \times \{2\pi\delta(\omega - \omega_1) + SB(\omega - \omega_1)\}$, where the function $G(t)$ reads $G(t) = \int d\omega e^{i\omega t} [1 + n_{\text{BE}}(\omega)] [J(\omega) - J(-\omega)]$, and the sideband follows as $SB(\omega) = \int dt e^{i\omega t} \{e^{G(t)} - 1\}$. For our spectral density of the lowest exciton transition $J(\omega) = S_1 * \gamma(\omega)$ we recover the shape of the vibrational sideband of [16].